

# Development and Calibration of the tracking Compton/Pair telescope MEGA

G. Kanbach<sup>1</sup>, R. Andritschke<sup>1</sup>, A. Zoglauer<sup>1</sup>, M. Ajello<sup>1</sup>, M. L. McConnell<sup>2</sup>, J. R. Macri<sup>2</sup>,  
J. M. Ryan<sup>2</sup>, P. Bloser<sup>3</sup>, S. Hunter<sup>3</sup>, G. DiCocco<sup>4</sup>, J. Kurfess<sup>5</sup>, V. Reglero<sup>6</sup>

<sup>1</sup> Max-Planck-Institut für extraterrestrische Physik, Garching, Germany

<sup>2</sup> Space Science Center, Univ. of New Hampshire, Durham, NH, USA

<sup>3</sup> Goddard Space Flight Center, NASA, Greenbelt, MD, USA

<sup>4</sup> IASF / CNR, Bologna, Italy

<sup>5</sup> Naval Research Lab., Washington, DC, USA

<sup>6</sup> GACE, University of Valencia, Spain

## ABSTRACT

We describe the development and tests of the prototype for a new telescope for Medium Energy Gamma-ray Astronomy (MEGA) in the energy band 0.4 - 50 MeV. As a successor to COMPTEL and EGRET (at low energies), MEGA aims to improve the sensitivity for astronomical sources by at least an order of magnitude. It could thus fill the severe sensitivity gap between scheduled or operating hard-X-ray and high-energy gamma-ray missions and open the way for a future Advanced Compton Telescope. MEGA records and images gamma-rays by completely tracking Compton and Pair creation events in a stack of double sided Si-strip track detectors surrounded by a pixelated CsI calorimeter. A scaled down prototype has been built and we describe technical details of its design and properties. Results from calibrations using radioactive sources and from measurements with an accelerator generated, fully polarized, gamma-ray beam are presented and an outlook to future plans with MEGA is given.

*Keywords:* DSSD tracking detector – CsI/PIN diode calorimeter – Compton telescope - gamma-ray astronomy - medium gamma-ray energies - MEGA

## 1. INTRODUCTION

Astronomy in the low to medium energy  $\gamma$ -ray range has always challenged the most advanced experimental techniques for two main reasons: (1) photon interaction cross-sections in the MeV range go through a minimum in their transition from the photoelectric effect ( $\sim 100$  keV) to pair creation ( $\sim 10$  MeV). In this so-called Compton range the interactions are characterized by small energy deposits and long-range secondary radiation. It is therefore necessary to build a "deep" detector to achieve a reasonable efficiency and to finely segment the detector in order to record and trigger widely separated interactions of the scattered photons. (2) the nuclear energy levels of all detector and structural materials lie in the MeV range and are therefore easily excited by energetic particles. The result of this systematic "radio-activation" in orbit is a prolific  $\gamma$ -ray background of local origin which must be effectively discriminated against to achieve a useful sensitivity for astronomical targets. COMPTEL [1] was the first instrument in space to explore this difficult spectral band. The results from COMPTEL opened a new window to the Universe and proved that a wide variety of astrophysical sources and processes can be studied best in the range from  $\sim 1$  to several  $10$ 's of MeV. Key science topics for this range are the investigation of cosmic high-energy accelerators, sites of active nucleosynthesis with  $\gamma$ -ray line emitting isotopes, and the mapping of large-scale structures in the Galaxy and beyond. Typical astronomical sources involve relativistic processes around compact objects like galactic or stellar mass black holes and neutron stars. Often extremely dynamic and explosive phenomena in the innermost environments of 'relativistic stars' (supernova explosions, gamma-ray bursts, accretion, and relativistic jets) lead to prolific emission of low energy gamma radiation. Since we expect many sources to be highly time variable or transient, an all-sky-survey type mission would be of great advantage to detect many sources and to maximize the scientific return. For a more detailed discussion refer to [6,7]. Telescopes based on the detection of Compton- and pair-creation-interactions have intrinsically large fields-of-view and are well suited as sky survey monitors and to map large-scale extended emissions. These extended sources of high-energy photons arise partly from interactions of cosmic-rays with interstellar gas, from dispersed radioactive isotopes (mainly  $^{26}\text{Al}$ ,  $^{60}\text{Fe}$ ,  $\beta^+$ -decay with following annihilation radiation), and possibly from the decay of dark matter in a galactic halo.

Presently the GLAST [2] mission, a third generation (after SAS-2/COS-B [3,4] and EGRET [5]) pair-creation telescope sensitive above 20 MeV, is scheduled to be launched in 2007. In Figure 1 the point source sensitivity, i.e. the minimum detectable flux, for past, present and future instruments in the low through high-energy regimes is shown. The lack of a sensitive instrument from 1-10 MeV is evident. It is therefore timely to develop a second-generation  $\gamma$ -ray telescope in the Compton energy range to maintain the overall multi-wavelength sensitivity, which is so important for a full understanding of high-energy astrophysics.

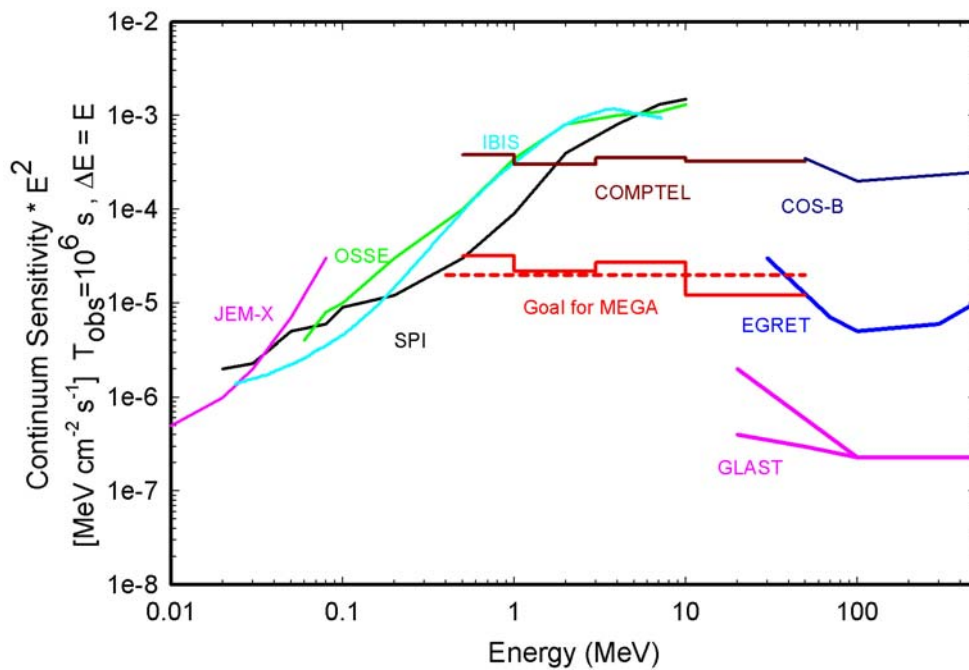


Fig. 1. Sensitivity levels for selected hard X- and  $\gamma$ -ray telescopes. The goal for MEGA is set to be about one order of magnitude improvement over COMPTEL (dashed line). The histogram for MEGA shows preliminary results of a simulation for a MEGA space mission.

The sensitivity goal for the next MeV spacecraft mission should fall half way, on a logarithmic scale, between the COMPTEL/INTEGRAL sensitivities and the extension of the GLAST sensitivity into the MeV range. A mission that attains this intermediate level of MeV sensitivity will not only follow the highly successful example of experimental progress in the range above 100 MeV, but

also could be realized long before a visionary Advanced Compton Telescope (ACT), corresponding to GLAST, is available. It will likely revolutionize MeV astronomy in the manner that EGRET revolutionized astronomy at 100 MeV.

To accomplish these goals with a medium sized mission requires new designs beyond that of COMPTEL and EGRET. We have been developing and testing such a design, called MEGA, for a new Compton / low energy pair telescope. MEGA functions in some ways similar to COMPTEL and EGRET, but also differs in many aspects. MEGA uses a stack of double-sided silicon strip detectors (DSSD) as a scattering and conversion tracking detector and finely pixelated CsI/PIN diode scintillation detectors for the absorption of the scattered radiation. A schematic of the basic MEGA design is shown in Fig. 2.

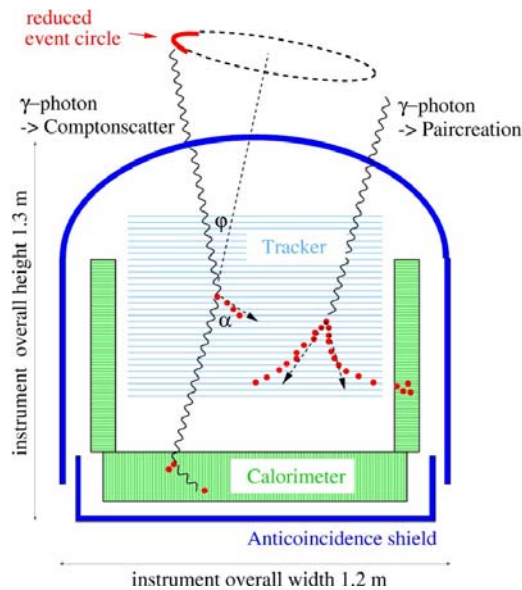


Fig. 2. Schematic of the MEGA instrument and kinematics of  $\gamma$ -ray interactions.

In this paper we present the implementation of this design in a prototype, its measured properties, our plans for testing the unit on a high-altitude balloon flight and the possible deployment of a telescope based on this concept on a medium-sized satellite mission.

## 2. MEGA PROTOTYPE

### 2.1 Principle of Operation

Two physical processes dominate the interaction of photons with matter in the medium-energy  $\gamma$ -ray band: Compton scattering at low energies, and electron-positron pair production at higher energies, with the changeover around 8 MeV for most detector materials. In both cases the primary interaction produces long-range secondaries whose directions and energies must be determined in order to reconstruct the incident photon. MEGA, like previous Compton and pair creation telescopes, will employ two separate detectors to accomplish this task: a tracker, in which the initial Compton scatter or pair conversion takes place, and a calorimeter, which absorbs and measures the energy of the scattered components (see Fig. 2). In the case of Compton interactions, the incident photon scatters off an electron in the tracker. The interaction position and the energy imparted to the electron are measured. The scattered photon interaction point and energy are recorded in the calorimeter. From the positions and energy deposits of the two interactions the incident photon scatter angle  $\varphi$  is computed from the Compton equation (1).

$$\cos \varphi = 1 + \frac{m_e c^2}{E_\gamma} - \frac{m_e c^2}{E_\gamma - E_1}, \quad (1)$$

The primary-photon incident direction is then constrained to an event circle on the sky. For incident energies above about 2 MeV the recoil electron usually receives enough energy to penetrate several layers, allowing it to be tracked. This further constrains the incident direction of the photon (the *reduced event circle* in Fig. 2).

The differential Klein-Nishina cross section for Compton scattering contains a strong dependence on the polarization of the incident  $\gamma$ -ray photon. Scattered photons are emitted preferentially perpendicular to the direction of the electric field vector of the incoming photon. The strongest azimuthal modulation in the distribution of scattered photons occurs for energies between 0.4-5 MeV (lower range of MEGA) and scatter angles of  $\sim 90^\circ$  and  $54^\circ$  respectively. This makes a Compton telescope with a calorimeter covering a large solid angle a unique polarimeter for  $\gamma$  radiation.

In the case of pair production, the incident photon converts into an electron-positron pair in the tracker. These two particles are tracked and determine the incident photon direction. The total energy is then measured through the deposits absorbed in the tracker and/or the calorimeter.

The design of a new high-energy  $\gamma$ -ray telescope must be based on numerical simulations as well as experimental detector developments. From the concept in Fig. 2 we used GEANT3 to develop the baseline for a satellite version of MEGA (Figure 3). In this version, the tracker contains 32 layers of double-sided Si detectors (thickness  $500\mu\text{m}$ , area  $6\times 6\text{ cm}^2$  each wafer,  $6\times 6$  wafers/layer, inter-layer spacing  $10\text{mm}$ ). The CsI calorimeter is  $8\text{ cm}$  deep on the bottom and  $4\text{ cm}$  deep on the side walls. The cross-section of each CsI element is  $5\times 5\text{ mm}^2$ . Structural material to hold the active detector elements (overall about 15% by mass) is included in the GEANT models and is based on a pre-phase A study of a possible MEGA satellite detector [18]. These choices led to the construction a representative prototype detector (also Figure 3) of about 25% of the area and 33% of the depth of the full satellite version. The prototype has been used to evaluate the performance characteristics in a series of calibrations. In the following sections we describe the prototype telescope components in more detail and present their properties in current experimental results.

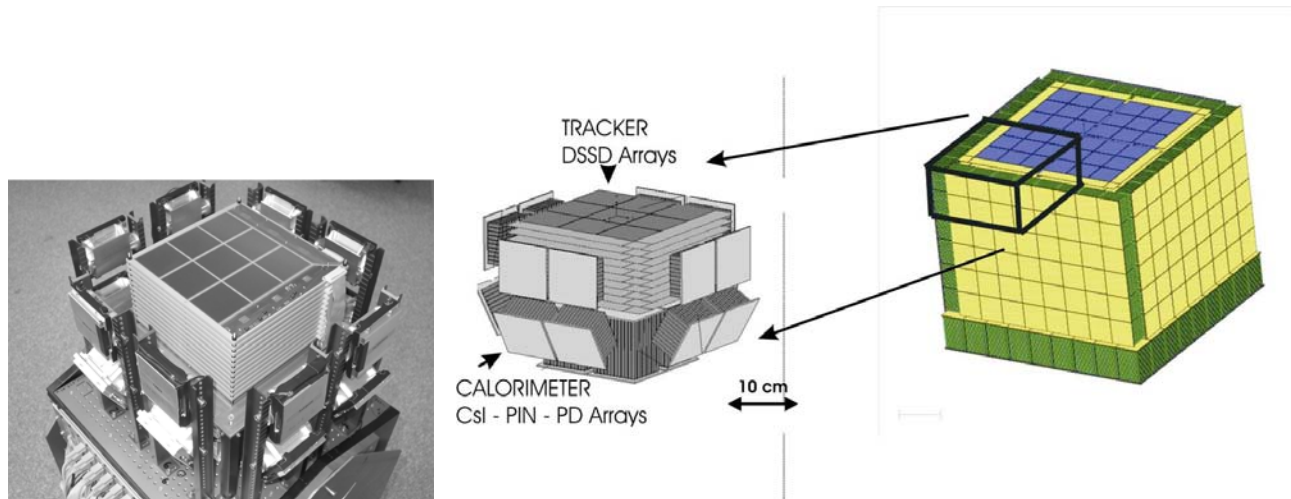


Fig. 3. The GEANT models for the MEGA satellite version (right), prototype (middle) and a photograph of the actual prototype detector (open to show the DSSD and CsI detectors).

## 2.2 MEGA components

### 2.2.1 The tracking detector

The tracker must accomplish several tasks. It must: (1) act as the scattering medium for Compton interactions; (2) measure the scattering location and the energy imparted to the recoil electron; (3) act as the conversion medium for pair production; (4) provide a large interaction volume for both processes to achieve good sensitivity; (5) record the tracks and energy deposits of all secondary particles, both electron-positron pairs and Compton recoil electrons; (6) provide a fast timing signal to be used in a coincident trigger with the calorimeter; and (7) operate without elaborate cooling and with reasonable power consumption. Thus good position, energy, and time resolution are required simultaneously in a large volume. The logical choice of detector technology for the tracker was a stack of double-sided silicon strip detectors (DSSD). The detectors used in the prototype were designed by the MPE semiconductor laboratory and produced by Eurisys Mesures, Lingolsheim, France. Each layer of the tracker is composed of a 3×3 array of 500 μm thick silicon wafers, each 6×6 cm<sup>2</sup> in size and fitted with 128 orthogonal p and n strips on opposite sides (470 μm pitch). The detectors are mounted in open frames machined out of PEEK material, such that wire bonds can be applied to both sides, and stacked with 10mm distance between layers. Overall the tracker's mass budget contains about equal amounts of active material (DSSDs) and structural material (frames, circuit boards); however inside the tracking volume the fraction of inactive holding structures to DSSDs is less than 10% by mass. The DSSD strips are biased using the punch-through principle and AC-coupled via metal strips separated from the strip implant by an insulating oxide/nitride layer. The strips from adjacent wafers ("ladder") in the 3×3 array are wire-bonded in series and read out by 128-channel TA1.1 ASICs<sup>1</sup>, creating a total area of 19×19 cm<sup>2</sup> position-sensitive area. At 20°C a typical energy resolution of 15-20 keV FWHM, a position resolution of 290 μm (measured with muon tracks), and a time resolution of ~ 1 μs is measured [15]. Contributions to the energy resolution (noise) come from the input capacitance (~25%), the leakage current (30-50%), and interference of unspecified origin on the read-out electronics. The stack in the MEGA prototype detector (Figure 3) contains 11 layers. Figure 3 also shows the front-end electronics

---

<sup>1</sup> Manufactured by IDE AS, Oslo, Norway

boards mounted next to the Si wafers. The tracker for the satellite size MEGA could be assembled from four quadrants, each similar to the prototype tracker, with the electronics on the outer rim.

### *2.2.2 The calorimeter*

The MEGA prototype calorimeter consists of 20 modules, each with an array of  $10 \times 12$  CsI(Tl) scintillator bars of cross-section  $5 \times 5 \text{ mm}^2$  read out with Silicon PIN-diodes and low-noise, self-triggering front end electronics (also TA1.1). The length of the CsI bars (the depth of the calorimeter) was chosen to correspond to the stopping power needed to absorb the scattered photons at different angles, i.e., large scatter angles produce low energy secondary photons that are stopped in thinner crystals while forward scattering requires a thicker calorimeter. The upper side wall modules are 2 cm deep, the lower side wall 4 cm, and the bottom calorimeter is 8 cm deep. The CsI(Tl) bars were manufactured by Hilger Crystals, U.K. and are polished on all sides. The bars are packed into the modules with optical separation using several layers of reflective paper (Millipore). The monolithic PIN diode arrays were manufactured by Hamamatsu (custom made for MEGA,  $10 \times 12$  square pixels of  $5 \times 5 \text{ mm}^2$  area, inter-pixel spacing  $700 \text{ }\mu\text{m}$ ) and are coupled to the scintillators with a prefabricated layer of transparent silicon cushions where the individual pixels are separated by a grid of opaque white silicon. The 8 cm modules are read out from both ends. The ratio of the two signals allows the localization of the energy deposit along the bar with a typical resolution of  $\sim 2 \text{ cm}$  (FWHM). This 3-d resolution, together with the size of the energy deposit, is important for reconstructing the correct sequence of multiple interactions in the calorimeter. The energy resolution of the calorimeter modules was measured with radioactive sources. Typical results for  $\Delta E/E$  (FWHM) at the incident energy of 662 keV range between 13% (for a 2 cm unit) and 14% (for 8 cm). Contributions to the energy resolution come from the intrinsic noise of the scintillator ( $\sim 1\%$ ), variations in light transfer and coupling ( $\sim 5\%$ ) and electronic noise sources ( $\sim 7\text{--}8\%$ , capacitance and interference). The energy resolution of the calorimeter is so far the limiting factor for the angular resolution of the MEGA design. Detectors with a decisively better resolution (e.g. new scintillators like  $\text{LaCl}_3(\text{Ce}^{3+})$ , segmented CZT or Ge) could very much improve the telescope imaging quality. A viable short-term development seems to be the application of Silicon drift detector diodes to replace the PIN diodes. This change could improve on the energy resolution of a CsI calorimeter by about a factor 2.

### 2.2.3 Electronics, Trigger processor, and Data acquisition

The MEGA prototype contains 8448 and 2880 channels of measurement in the tracker and calorimeter respectively ([8], [9], [16]). A satellite telescope with the same pixelation will contain more than ten times this number of data channels. It is evident that the data acquisition from this large number of channels demands highly integrated, low power electronics already in the prototype stage. Figure 4 shows a schematic block diagram of the readout electronics and data acquisition system of the prototype detector.

The front-end, repeater card, opto-coupler, trigger processing card and power supplies for the detectors are custom developments. The sequencer, analog-to-digital converters, and an on-board computer (OBC) with mass storage (10+40 GB hard disk), is based on commercial VME modules. The data acquisition and detector control software is based on C++ and the ROOT software library from CERN. It is implemented and operates on a PC Linux system (Pentium III, 700 MHz) of the OBC.

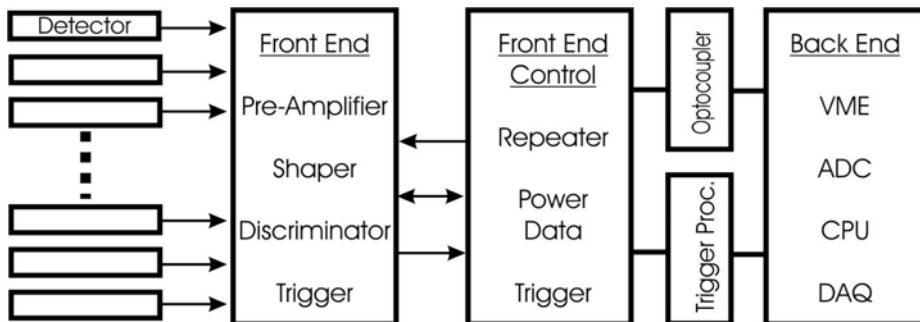


Fig. 4. Schematic block diagram of the MEGA readout electronics and data acquisition system

In the front-ends of both the tracker and calorimeter, we use VLSI amplifier-ASIC's of type TA1.1 custom designed by IDE with built-in trigger capability. This ASIC features the following characteristics: (1) low noise level of  $165 e^- + 7 e^-/pf$  with an adjustable shaping time (1-3  $\mu s$ ); (2) a dynamic range of  $\pm 5$  MIPs; (3) 128 channels in parallel with serial readout up to 10 MHz clock rate; (4) low power consumption of  $\sim 1.5$  mW/channel (5) common trigger output from 128 level discriminators with common adjustable threshold; and (6) a 128 bit blocking register to prevent individual noisy channels from triggering.

So-called repeater cards supply 3 ASICs each with low noise power, shift and amplify logic and analog signals, and generate the (analog) trigger threshold levels. All signals pass through opto-couplers to galvanically isolate the front-ends, which are on different bias potentials, against each other and the rest of the system.

The trigger signals of each chip are routed to the trigger processing unit. Up to 60 triggers are combined into 20 subunit triggers, i.e. 12 (only 11 in use) tracker layers and 8 groups of calorimeters. A first level coincidence is formed by the occurrence of a tracker and a calorimeter signal within a trigger window of about 3  $\mu$ sec duration. This is a rather long window, which was demanded by the slow response of the calorimeter scintillators and the layout of the TA1.1 ASICs, which are not equipped with a separate fast trigger output. While the problem of accidental coincidences of unrelated interactions is not a major concern in the small prototype detector, we have to develop a much faster triggering scheme for a future satellite detector. As mentioned above, more advanced ASICs feature fast and temporally accurate trigger circuitry. Together with the second level trigger (described below) using coarse information on the distribution of the energy deposits, e.g. whether a track has been generated, the level of undesirable chance coincidence events can be effectively controlled also for a larger instrument. An absolute veto and a programmable veto are also foreseen for the anticoincidence shield, which is necessary on a balloon flight (see chap. 4.1). If no absolute veto is detected, a 21-bit word is generated from the 20 subunits plus the programmable veto taking account of the different timing behaviors of the three detector types. The word is used as an address to interrogate a 2 Mbit RAM where the valid, i.e. coincident, trigger combinations are stored as non-zero bits. The flexibility to generate different memory loads allows more or less stringent trigger conditions and therefore an restriction to higher quality events for an optimal use of the limited readout rate. Valid patterns initiate a readout sequence, which is generated by the sequencer card. It starts with a hold signal indicating the front-end ASICs to store the pulse heights of all its channels. Then the sequence continues to address each channel (8 in parallel, up to 1536 in series) and digitizes its pulse height. The final reset restores the readiness for the next event. Finally, the data set generated for each event is stored with a GPS based time-stamp in the OBC storage medium. Housekeeping information is also stored at regular intervals. Current readout rates of the prototype are limited to less than  $\sim 120$  events/s. We plan to use the adjustable trigger conditions to accommodate and trim the expected trigger rates on

the planned balloon flight. The predictions for the rates at balloon altitudes are not yet available, because some components of the balloon payload (e.g. anticoincidence detector ) have not yet been fully integrated on the system.

#### *2.2.4 First level data processing and event reconstruction*

The basic data are stored as sets of “hits” (channel numbers and pulse height information) for each event in the detector. The data processing developed for MEGA and described in more detail by Zoglauer et al. [17] can only be summarized here. Initial data processing converts each hit into a position and energy measurement based on the detector geometry and calibration. The aim of the subsequent event reconstruction is to identify the type of interaction process, such as Compton scatter, pair creation, charged-particle track, etc., and to reconstruct the origin and energy of the photon. This algorithm has the following steps:

(i) Search for pair events, where “ $\Lambda$ ”-shaped structures indicate the vertex of an electron-positron pair.

(ii) Search for high-energy charged particles (muons, protons or high-energy electrons), which appear as nearly straight tracks from tracker to calorimeter and which normally have additional hits or tracks. These background events are rejected from further analysis.

(iii) Separate Compton events from the remaining data: (i) identify the direction of motion of an electron track, (ii) determine the overall Compton sequence and (iii) finally check, if the event can be accepted as a Compton event, i.e. a reasonable reconstruction can be achieved. Multiple interactions in the tracker or calorimeter can of course be accepted as valid events. For example at a photon energy of  $\sim 2$  MeV we find less than 5% of the events as multiple interactions in the tracker; in the larger satellite geometry this category could be populated by about 15% of all events.

We emphasize that in a tracking gamma-ray telescope like MEGA, the track itself is one of the most valuable elements to identify the event type and the sequence of interactions. The track normally gives the starting point of an event and considerations of absorption probabilities etc. lead to a reduction of random coincidences as well as to the correct sequencing of good events. It is one of the main goals of the envisaged balloon flight exposure to test this ability of background control in the MEGA prototype.

### 3. CALIBRATION MEASUREMENTS

From January to March 2003 the prototype was calibrated with laboratory sources ( $^{22}\text{Na}$ ,  $^{137}\text{Cs}$ ,  $^{88}\text{Y}$ ) in the near-field, and in April/May 2003 it was calibrated at the High Intensity Gamma Source HI $\square$ S ([10]) at Duke University (Durham, North Carolina) in the far-field. The latter calibration used monoenergetic ( $\Delta E/E < 2\%$ ) and 100% polarized pencil beams at different energies (0.7, 2, 5, 8, 10, 12, 17, 25, 37 and 49 MeV) and different angles of incidence ( $0^\circ$ ,  $30^\circ$ ,  $60^\circ$ ,  $80^\circ$ ,  $120^\circ$ ,  $180^\circ$ ). Based on these data, preliminary imaging properties of the telescope have been determined.

The image reconstruction is performed with an unbinned maximum-likelihood method called list-mode maximum-likelihood expectation maximization, which originally was developed for medical imaging with SPECT cameras ([11]) and later was adapted for use in astrophysics ([12]). This method allows the incorporation of different event types (tracked and untracked Compton events as well as pair events) into one image while preserving all measured information.

#### 3.1 The Compton Scatter Regime and its imaging response

Ideally, a tracking Compton telescope should measure all parameters to directly calculate the origin of the incoming photon: direction and energy of the scattered photon as well as direction and energy of the recoil electron. Below 2 MeV the energy of the electron is in most cases not sufficient to generate a track in D1, the DSSD stack. For these ‘untracked events’ the origin of the incident photon can only be restricted to the classical cone section, which is represented by circles in the far-field and ellipses/hyperbolas in the near-field (see Fig. 2). Both lead to a large ambiguity of the origin of these photons. The width of this cone section is mainly determined by the energy measurement. If, on the other hand, the Compton scattering imparts enough energy to the recoiling electron and releases it from its layer of origin a ‘tracked event’ results. The momentum vector of the particle can then be estimated. However the accuracy of the initial electron direction is limited by energy dependent Molière (small-angle) scattering in the silicon and the incident photon direction cannot be restricted to a single vector: The knowledge of the cone section, determined by the measured energies, in combination with the electron track, however restricts the possible origins of the photon to short arcs of the cone section, as seen in Fig. 5. The length of these arcs (FWHM) for tracked events was measured in the beam calibration as  $33^\circ$ ,  $17^\circ$ , and  $15^\circ$  at 2, 5, and 8 MeV

incoming beam photon energy respectively. If one would choose thinner DSSD layers, e.g. reduce the presently used 500  $\mu\text{m}$  Si detectors to 300  $\mu\text{m}$ , the angular dispersion on the electron tracks could be further reduced to about 75% of the above values. This option however would require a correspondingly larger number of layers (and detector channels) in order to maintain the efficiency of the telescope.

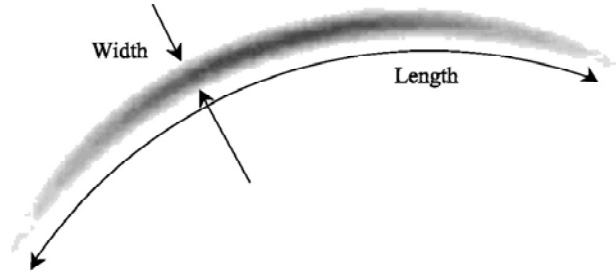


Fig. 5. The possible incident directions of tracked  $\gamma$  rays are restricted to an arc (schematic).

### 3.1.1 Angular Resolution.

One method of characterizing the width of the response and therefore the angular resolution is the Angular Resolution Measure (ARM). It is defined as the difference between the real and the measured Compton scatter angle. Examples are given in Fig. 6. This distribution for all events contains tracked as well as untracked events at  $2.0 \pm 0.2$  MeV and has a FWHM of  $7.4^\circ$ . If only untracked events are considered, the shape is narrower ( $6.2^\circ$ ), whereas tracked events produce a broader ARM ( $13.4^\circ$ ). This behavior is expected, since tracked events suffer especially strongly from the limited energy resolution in the calorimeters: Tracks are only generated if sufficient energy is transferred to the electron. This results in scattered photons of lower energy and deposits in the calorimeter have a correspondingly larger relative energy error for these scattered  $\gamma$ -rays. This error is most important for the error in the Compton scatter angle  $\phi$  at large scatter angles. If we compare this result with the final calibration of the COMPTEL satellite instrument [1] we find e.g. that the COMPTEL ARM value at 2 MeV was  $\sim 3.6^\circ$  FWHM. The differences between the MEGA prototype and COMPTEL are caused by (i) the large scale ( $\sim 1.5\text{m}$ ) of COMPTEL with good spatial resolution of the interactions which provides a good direction of the scattered photon and (ii) the good energy resolution in the COMPTEL calorimeter of e.g.  $\Delta E/E \sim 7\%$  (FWHM) at 2 MeV.

With the current and still preliminary energy resolution of the MEGA prototype, which was measured e.g. in the 8 cm bottom calorimeters at  $\Delta E/E \sim 14\%$  at 662 keV, the angular resolution for tracked events is far away from the physical limit, which is given by Doppler-broadening. At 2 MeV Doppler-broadening would only lead to an average width of  $\sim 0.2^\circ$  in Silicon [13]. Therefore improvement of the energy resolution of the calorimeter is crucial for the performance of a tracking Compton telescope.

The angular resolution of recorded Compton events as a function of the energy first improves from threshold to about 2 MeV (untracked events FWHM ARM  $\sim 6^\circ$ ) and then deteriorates again for higher energies. At lower energies the measurement errors of the energy are dominant while at high energies incomplete absorptions start to be important: The scattered photons leak and the electrons are no longer stopped in the tracker. Nevertheless, incomplete absorption will be much less pronounced in the larger satellite geometry with its more compact calorimeter [14].

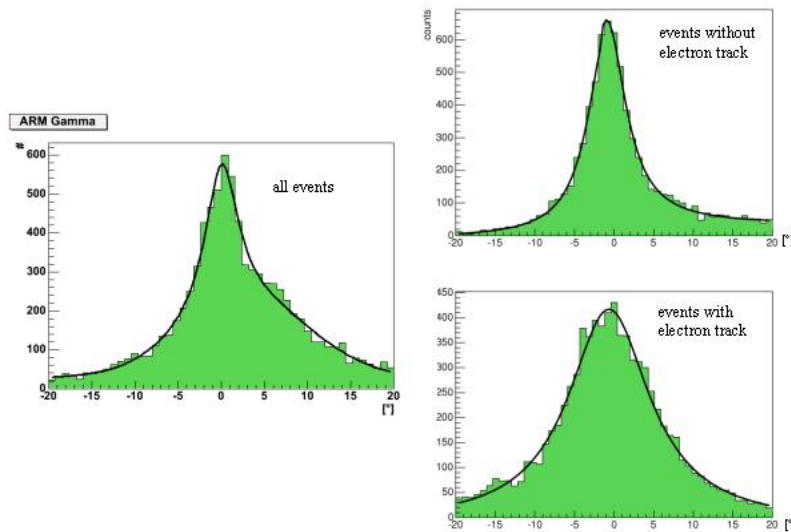


Figure 6. ARM distributions of tracked and untracked events from 1.8 to 2.2 MeV (FWHM of  $\sim 7.4^\circ$ , all events).

### 3.1.2 Direction of motion for Electron Tracks

The most important characteristic of a tracking Compton telescope is the electron track. Using  $\gamma$  rays from a 1.8 MeV  $^{88}\text{Y}$  source the HWHM of the track direction distribution is  $\sim 42^\circ$ . This is

close to the physical limit given by Molière scattering. At this relatively low energy more than 85% of all tracks, which penetrate on average 2.5 layers, can be reconstructed correctly within the limits stated above. The electron tracking performance also depends on the length and inclination angle of the track. The recovery of the correct direction of longer tracks, e.g. 4 layers and above, is achieved in 90% of all cases. This was verified in the beam calibrations.

### 3.1.3 Polarization.

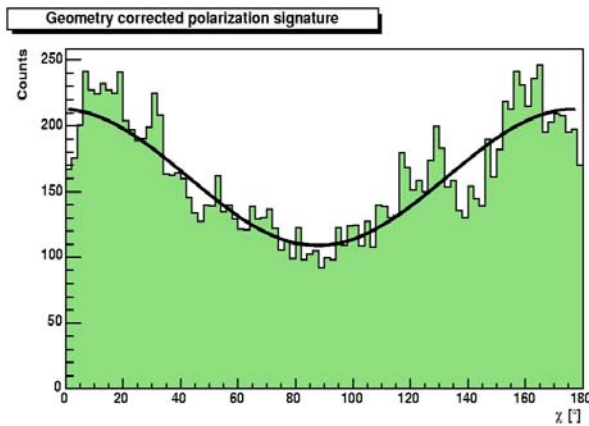


Fig. 7. Geometry corrected event distribution of the azimuth scatter angle for

large scatter angles. MEGA with its geometry (see Fig. 2) is well suited to detect polarization. Fig. 7 shows a polarization signal. The measurement was performed with 100% polarized 710 keV  $\gamma$ -rays produced at the HI $\gamma$ S facility at Duke University. The  $\gamma$ -rays are produced by Compton backscattering of storage ring electrons on optical laser photons and are therefore completely polarized. The asymmetries and response of the instrument to an unpolarized beam is used to correct the measurements of a polarized beam. To measure this unpolarized response we used a  $^{137}\text{Cs}$  source (662 keV) positioned one meter above the detector. Registered events with unphysically large energies were discarded from the analysis. The azimuth angles of the scattered photons are determined for each detected event, corrected for the detector asymmetries and fitted with a sinusoidal signal. The modulation factor  $\mu$ , which gives the degree of polarization, is defined as

Most processes in high-energy astrophysics can generate polarized  $\gamma$ -radiation (e.g. synchrotron radiation, bremsstrahlung, Compton scattering, etc.). Polarization measurements are therefore of great value in understanding the emission mechanisms of  $\gamma$  rays. The Compton cross section is polarization-dependent and has its strongest signature, a sinusoidal modulation in the azimuthal distribution (see sect. 2.1), at

$$\mu = \frac{N_{\max} - N_{\min}}{N_{\max} + N_{\min}}, \quad (2)$$

where  $N_{\max}$  and  $N_{\min}$  are the number of counts at the maximum and the minimum of the azimuth angle distribution. From the 100% polarized beam of the Duke measurement this modulation factor was measured to be  $\mu_{100} = 0.30 \pm 0.08$  (Fig.7) [14]. The error is statistical and  $\mu$  was not corrected for any time-varying detector response. An additional correction for the divergent  $^{137}\text{Cs}$  beam adjusts the value to  $\mu_{100}^{\text{corr}} = 0.30 \pm 0.03$ . Monte Carlo simulations predict a modulation of  $\mu_{100} = 0.304$ . The geometry of the instrument/beam setup should produce the maximum of the distribution (polarization angle) at  $0^\circ$  - the maximum was measured to be at a compatible  $-4.6^\circ \pm 2.1^\circ$ . Other measurements at 2 MeV with poorer statistics show a modulation of  $\mu_{100}^{\text{corr}} = 0.13 \pm 0.04$ , also in agreement with the simulations [14].

#### 3.1.4 Multiple and Extended Sources.

In a realistic astrophysical environment a telescope must detect and resolve multiple sources within the field of view. To test the instrument capability to do this we placed five sources of different energies with different intensities at different positions in the field of view of MEGA. All five sources (not shown here, see fig 8 in [14]) were reconstructed at the correct positions. In space it will also be necessary to resolve extended sources such as supernova remnants, OB-associations or molecular clouds. This ability was demonstrated by a measurement, where two  $^{88}\text{Y}$  sources were mounted on a rotating propeller located 27 cm above the center of the tracker. The sources moved in a circular path of radius 7 cm. The reconstructed image is shown in Fig. 8. This corresponds to an angular diameter of  $\sim 29^\circ$  at infinity. The image contains 138,000 Compton events in the energy range from 0.8 to 1.0 MeV. The non-uniformities of the image are artifacts of the non-uniformities of the instrument response, an effect that should be correctable.

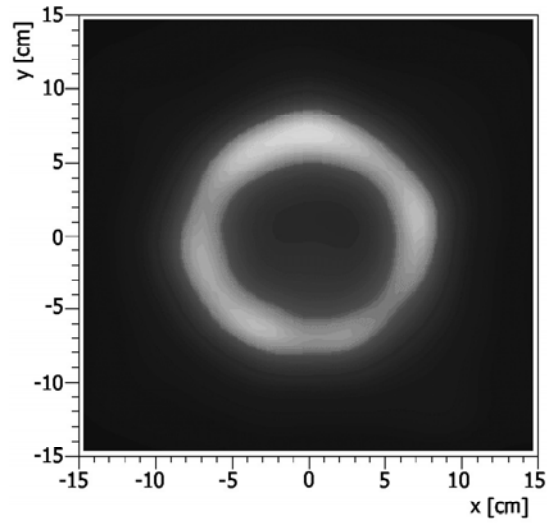


Fig. 8. The time-averaged image of two  $\gamma$ -ray sources moving in a circular path in the field of view.

### 3.2 Pair-production regime

In silicon the dominant reaction for  $\gamma$  rays is pair production once the photon energy exceeds 8 MeV. MEGA can track the electron-positron pair and determine the incident energy and direction.

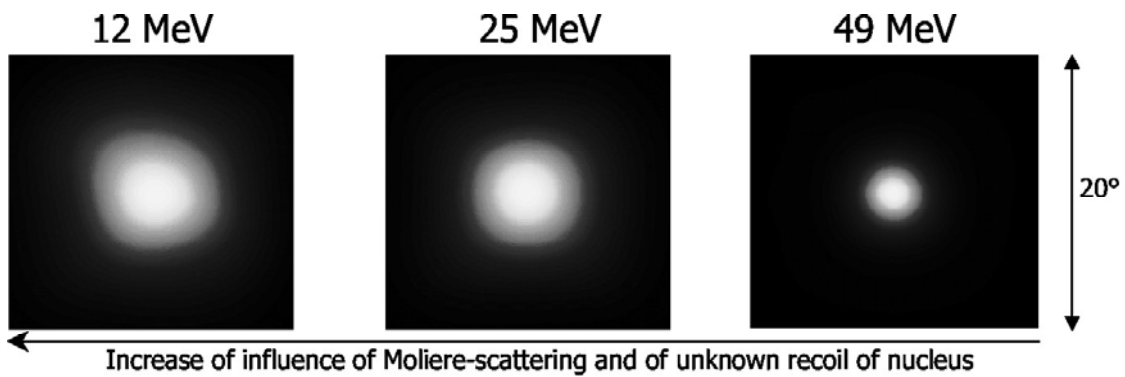


Fig. 9. Measured angular resolution in the pair mode.

### 3.2.1 Angular Resolution.

The angular resolution of pair events is dominated by small angle Molière scattering of the electrons in the DSSDs and the unmeasured recoil of the target nucleus. The influence of both effects is greatest at threshold (8 MeV) and diminishes thereafter as illustrated in Fig. 9 from calibration data. The angular resolution, given as the cone half-angle, which contains 68% of all events, is illustrated in Fig. 10. At 49 MeV it is roughly 2× better than in the EGRET telescope. At energies below 100 MeV it will also surpass the expected performance of GLAST and AGILE, because these telescopes contain passive converter foils of considerable depth, which scatter the low-energy electrons strongly.

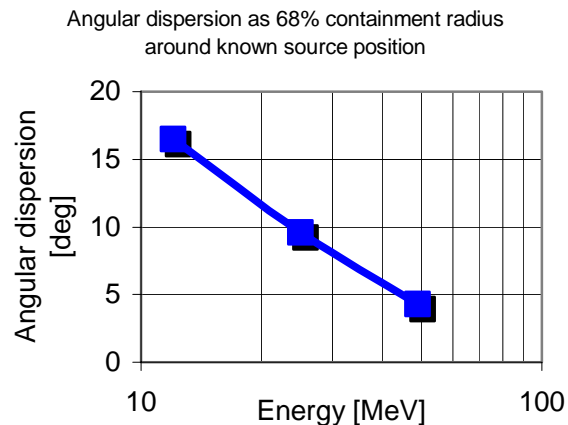


Fig. 10. Preliminary angular resolution curves for MEGA in the pair creation energy range.

### 3.3 Calibration Summary

This calibration demonstrated that the MEGA technique of detecting gamma rays works for a large energy range (from 500 keV up to 50 MeV) over a wide field of view. It also shows that MEGA can detect polarization up to at least 2 MeV. In the pair regime the telescope has excellent angular resolution.

Poorer angular resolution was measured in the Compton regime, because it is dominated by the poor energy resolution of the calorimeters. However, an improved version of the calorimeter is under development to improve the energy resolution (at least 2×) and lower the thresholds (at least

3×). Simulations show, that with drift-diodes in the larger satellite geometry, with a more compact calorimeter, an angular resolution for tracked events of  $\sim 2^\circ$  at 2 MeV is achievable.

## 4. FUTURE

### 4.1 Preparation of a balloon experiment

The prototype is being prepared for a high-altitude balloon flight to measure the background in a high-background radiation environment. We distinguish this part of the program by renaming the instrument MEGABALL. The MEGA prototype telescope is the core of the payload shown in Fig. 11. It will be surrounded by an anticoincidence shield (ACS) (Fig. 12) to reject charged particles of

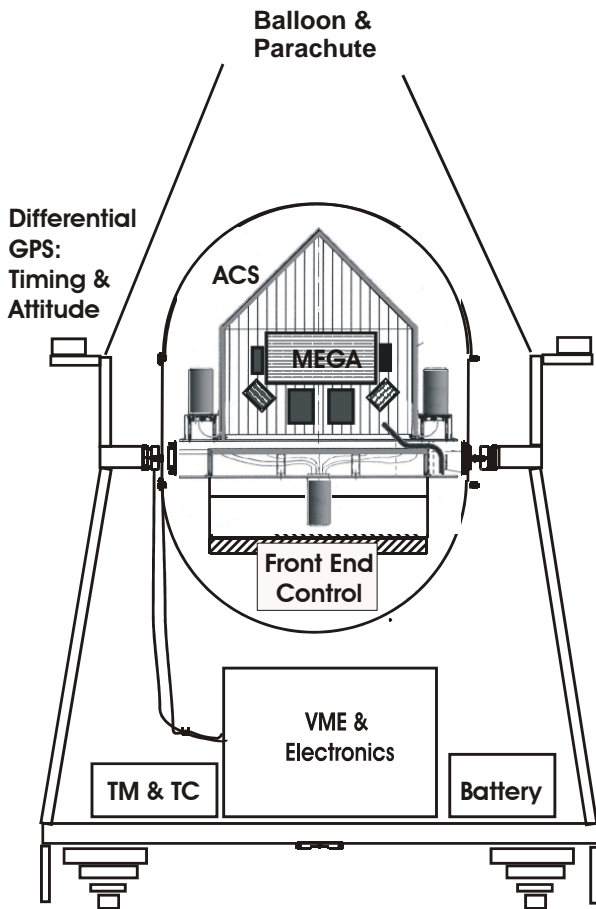


Fig. 11. The general layout of the MEGABALL balloon

cosmic and atmospheric origin. The ACS is made of 1.25-cm plastic scintillator plates (Bicron BC 412) and the scintillation light is measured by PMTs interfaced to wavelength shifting fibers that are optically coupled to the scintillator. Tests with radioactive sources and cosmic ray muons have shown that the ACS has a nearly uniform response and a particle rejection power of better than  $5 \times 10^{-3}$ . The telescope and the front-end electronics, including the repeaters and opto-couplers, are housed in a pressure vessel. A second pressure vessel encloses the back-end and command electronics. The attitude of the telescope is not actively controlled but is frequently measured with a differential GPS system. The GPS will also provide the absolute time to be imbedded in the event records. The present plans are to fly

MEGABALL from a base of the National Scientific Balloon Facility (NSBF, Texas or New Mexico) in 2005.

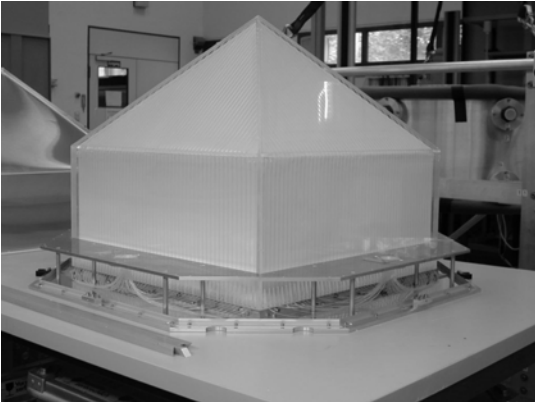


Fig. 12. The charged-particle shield detector (ACS) outfitted with wavelength-shifting fibers

#### 4.2 A MEGA Satellite Mission

A mission built around a  $\gamma$ -ray telescope like MEGA should fit well within a NASA MIDEX envelope in terms of mass, power, and cost. The ideal orbit of a MEGA mission should be a circular low altitude ( $\sim 500$  km) equatorial orbit. The advantage of such an orbit is that the spacecraft and instrument avoid the South Atlantic Anomaly, greatly minimizing the activation of material on the satellite. A constantly zenith pointing attitude of the telescope would on one

hand avoid the  $\gamma$ -ray emission of the earth's atmosphere and on the other generate a fairly uniform exposure as the wide field of view sweeps across the sky. Both internal activation and albedo  $\gamma$ -rays played major roles in limiting the sensitivity of COMPTEL. Except for the celestial poles, the sky will get complete coverage without the complexity of regular attitude control and pointing. Furthermore the regular scanning will allow for a very effective all-sky monitoring of unexpected transient sources. Dedicated pointings for bursts and targets of opportunities may still be possible at the expense of complicating spacecraft operations and spacecraft complexity. Simulations for a MEGA mission (shown as a histogram in Fig. 1) indicate that this concept can achieve the desired sensitivity levels for the next step in low- to medium-energy gamma-ray astronomy.

#### REFERENCES

- [1] Schönfelder, V. et al. *ApJ Suppl.* **86**, 657 (1993)
- [2] Michelson, P. et al., *AIP Conference Proceedings* **587**, 713 (2001)
- [3] Derdeyn S.M. et al. *Nucl. Instr. Meth.* **98**, 557 (1972)
- [4] Bignami, G.F. et al. *Space Sci. Instr.* **1**, 245 (1975)
- [5] Kanbach, G. et al. *Space Sci. Rev.* **49**, 69 (1988)
- [6] Kanbach, G. et al. *Proc. SPIE* **4851**, 1209 (2003)
- [7] Ryan J.M. et al. *Proc. SPIE*, Glasgow (2004), in press

- [8] Andritschke, R., Diploma thesis TUM (in German)<sup>2</sup> (2000)
- [9] Schopper, F., PhD thesis TUM (in German)<sup>2</sup> (2001)
- [10] Litvinenko, V.N. et al. *SPIE*, **2521**, 55, (1995)
- [11] Wilderman, S.J. et al. *IEEE Trans. Nucl. Sci.*, **45**, 957 (1998)
- [12] Zoglauer, A., Diploma thesis TUM (in German)<sup>2</sup> (2000)
- [13] Zoglauer et al. *Proc. SPIE* **4851**, 1302 (2003)
- [14] Zoglauer et al. in *Proc. IEEE, Portland 2003, Nucl. Sci. Symp. Conf. Rec., IEEE* (2004)
- [15] Bloser, P.F. et al. *NIM A*, **512**, 220, (2003)
- [16] Andritschke, R. et al. in *Proc. IEEE, Portland 2003, Nucl. Sci. Symp. Conf. Rec., IEEE* (2004)
- [17] Zoglauer, A. et al. *New Astron. Rev.* **48** 231 (2004)
- [18] Daimler-Chrysler Jena Optronik (DJO), Germany: 'Pre-Phase A study for MEGA' (2000)<sup>2</sup>

---

<sup>2</sup> available from <http://www.mpe.mpg.de/gamma/instruments/mega/www/mega-documents.html>